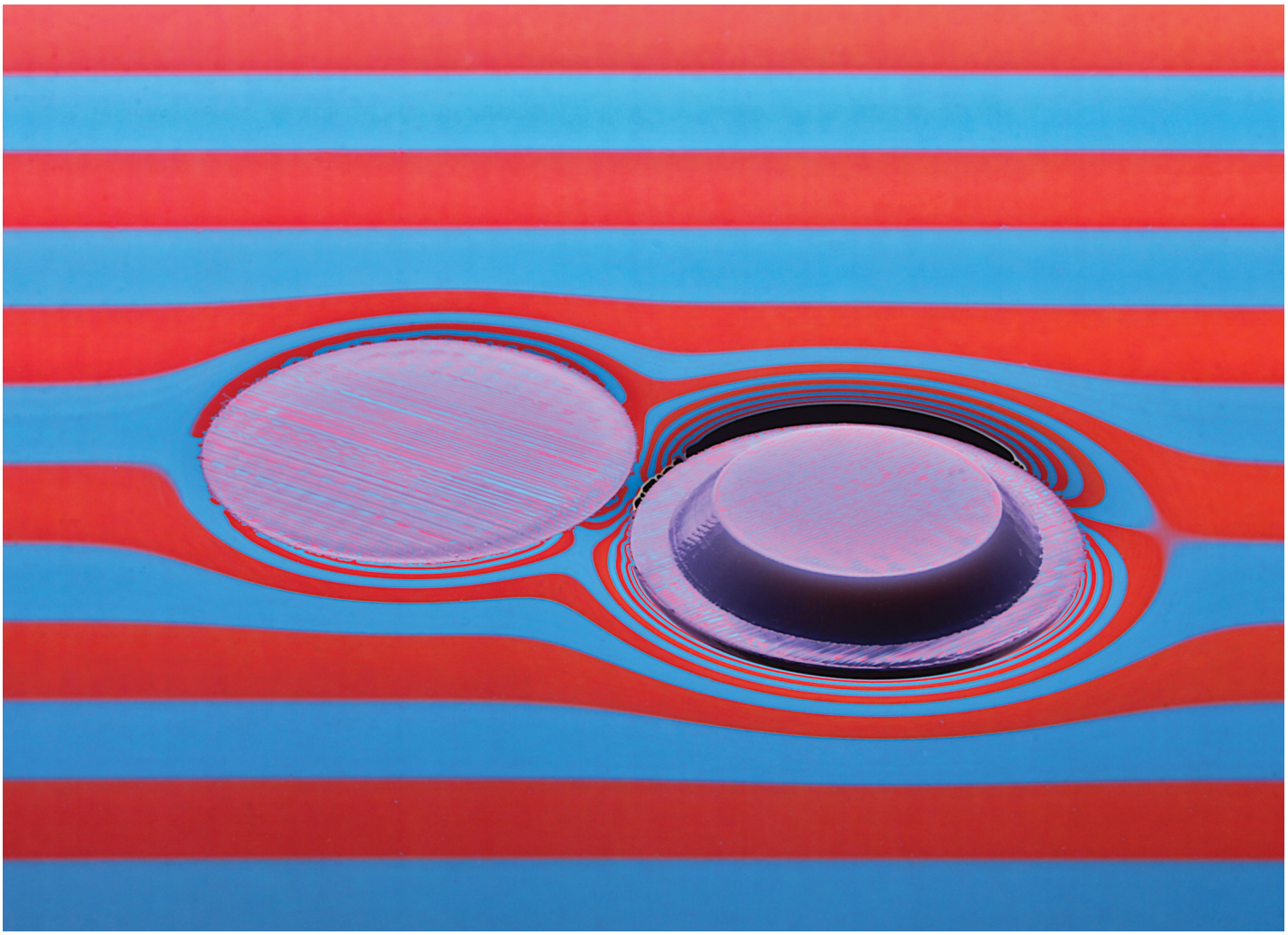

Highlighting research from the GRASP lab in the CESAM research unit from the University of Liège, Belgium.

Equilibrium distances for the capillary interaction between floating objects

Floating objects deform the surface of the water and interact due to capillary forces. We show that, in addition to attraction and repulsion, an equilibrium distance between these objects can occur. We propose a model for this effect, supported by experimental confirmations.

As featured in:

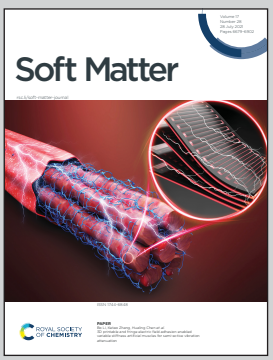

See Martin Poty and Nicolas Vandewalle, *Soft Matter*, 2021, **17**, 6718.

ROYAL SOCIETY OF CHEMISTRY

rsc.li/soft-matter-journal

Registered charity number: 207890

Soft Matter

PAPER

Cite this: *Soft Matter*, 2021, **17**, 6718

Equilibrium distances for the capillary interaction between floating objects

Martin Poty and Nicolas Vandewalle *

When small objects are placed at a water–air interface, attractive and repulsive interactions appear due to liquid deformations. Although it is commonly admitted that two floating objects deforming the liquid interface in the same way are only attracting, we show that in the case of objects whose height does not vary during the interaction, the situation is much more complex than expected. In fact, attraction and repulsion can coexist at different ranges, so that equilibrium distances are observed. A 1D model based on the capillary interaction between vertical plates immersed in water is used to illustrate and calculate these situations, giving a picture of capillary interactions. We show that the wetting condition plays a determinant role in the behaviour of the interaction between floating objects. We also demonstrate that the equilibrium distance is given by the logarithm of the capillary charge ratio, using the right capillary charge definition. We also discuss the particular case of the existence of an interaction with a zero-capillary charge. A general equation of the equilibrium distance is proposed. An experimental confirmation of this relation is also given.

Received 23rd March 2021,
Accepted 14th June 2021

DOI: 10.1039/d1sm00447f

rsc.li/soft-matter-journal

1 Introduction

When small objects or particles are placed along liquid–air interfaces (or more generally fluid–fluid interfaces), they interact due to capillary forces, originating from the interface deformations around each floating body. This effect has been studied since the article of Nicolson about the attraction between bubbles due to the buoyancy.[1] Then, this effect has been studied in various domains, including the self-assembly at liquid interfaces,[2–8] the building of micro swimmers on a free surface[9,10] or various biological phenomena.[11,12]

A few models have been proposed to describe the capillary attraction of identical particles.[13–18] Gifford and Scriven described the interaction between horizontal cylinders.[13] More recently, Vella and Mahadevan rationalized this interaction for spherical objects[14] and vertical cylinders.[15] Kralchevsky *et al.* considered another approach,[16–18] using the capillary charge as the characteristic depth of the liquid deformation close to each object. As opposed to what happens with the interaction between electric charges, the interaction strength between capillary charges is given by their product. Thus, the capillary force is attractive between objects of the same capillary charge and repulsive between objects with opposite capillary charges. Recently, Ho *et al.* measured this attractive force between floating disks.[19]

While the attractive or repulsive behaviour seems valid for small objects with respect to the capillary length, some simple experiments involving larger objects can show more complex behaviours. One of these experiments is shown in Fig. 1(a). The picture is made using the technique described in ref. 20 to show the deformation of the water. A light pattern is reflected on the water surface, and the deformations of the surface are translated into deformations of the pattern. The picture shows two 3D printed squares floating on water. Their sides are 6 cm and their thickness is 2 mm. The edges of the squares are wedge-shaped to pin the contact line. The one on the left is built with a bump to be heavier and therefore float at a greater depth than the one on the right. We can observe that the objects attract but without making contact. Since these objects have a negative capillary charge, they should attract each other, but a short-range repulsion provides a non-zero distance of equilibrium.

Another case appears during the self-assembly of multipolar objects. In a recent paper,[21] we build rhombi with opposite curvatures along their diagonals. In this way, once placed on the surface of the water, they create capillary charges localized at their tips, each rhombus having two positive charges and two negative capillary charges. This allows them to interact with each other to form ordered structures (see Fig. 1(b)).

According to the vast majority of previous studies,[1,13–18] the origin of the force between floating objects is a combination of the effects of surface tension and gravity. The surface tension causes a deformation of the liquid interface around the floating objects. Then the objects move to reduce their gravitational

GRASP, CESAM Research Unit, Institute of Physics B5a, University of Liège, B4000 Liège, Belgium. E-mail: nvandewalle@uliege.be

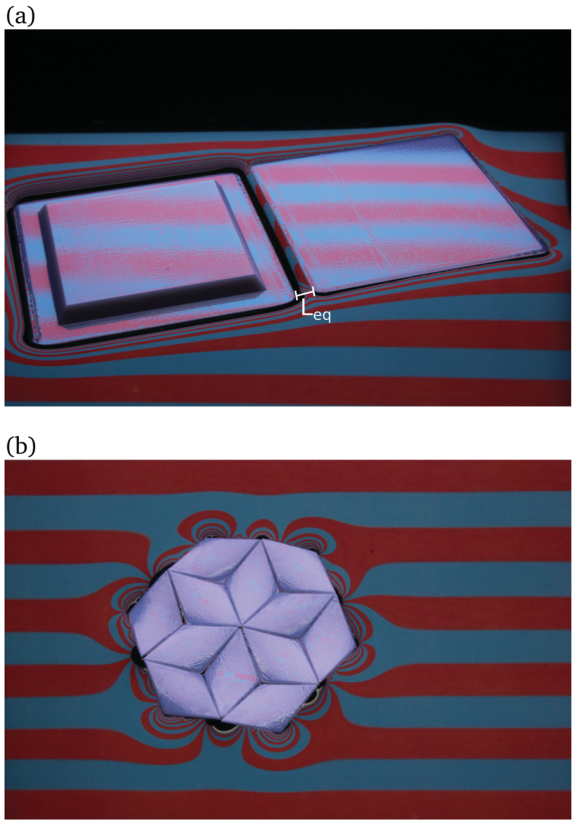

Fig. 1 (a) Picture of two squares floating on water and pinning the contact line at different depths. An equilibrium distance, highlighted as L_{eq}, is visible. The scale is given by the side of the square measuring 6 cm. (b) Picture of a self-assembly of floating rhombus-shaped components having positive and negative capillary charges located on the tips. They were extensively studied.[21] The scale is given by the sides of the rhombi measuring 1 cm. These pictures were taken using the method described in ref. 20.

potential energy in that modified energy landscape. For example, the attraction appears because the liquid meniscus deforms in such a way that the gravitational potential energy of both particles decreases when they approach each other. One could say that an object falls into the deformation created by the other and *vice versa* causing their attraction. This explanation implies that during the attraction, the height of the objects must necessarily vary. However in the case of Fig. 1(b), this explanation cannot be satisfactory. Indeed, each object has both positive and negative capillary charges. Those floating objects cannot realistically increase their vertical position during the attraction between positive capillary charges while, at the same time, decreasing it during the attraction between negative charges. So the interaction must be caused by some other effect. The common feature of the experiments shown in Fig. 1 is the fact that the depth of the objects remains constant. This can be explained by the large size of the objects in the first experiment compared to the capillary length. Dixit and Homsy[22] showed that for small bond numbers, the interaction is primarily driven by gravitational potential energy, while it is not the case for large bond numbers. The objects are large enough compared to the characteristic length of the deformation they cause that they cannot actually fall in the deformation caused by each other. Thus, we consider that the floating depth of a large floating object is always equal to the depth at which this object would float without being perturbed by another one. Small multipolar objects can also show situations where they cannot change their vertical position because of other multipolar surrounding objects as shown in the second example ref. 21 or in ref. 3,4,5,23. More examples can be found as in the situation studied by Kralchevsky *et al.*[16] where objects are placed on a substrate underwater.

While earlier works studied the apparition of an equilibrium distance between floating objects,[24,25] the aim of the present study is to introduce a new explanation for the capillary interactions between floating objects whose vertical position cannot vary during the interaction and characterize these interactions. We will show how objects of this kind can still interact without changing their vertical position and exhibit a more complex behaviour than simple attraction or repulsion. We will identify the conditions under which the non-zero equilibrium distances takes place. A complete picture will be given for idealized structures depending on boundary conditions, *i.e.* wetting properties of these objects. An experimental confirmation of the result will also be given.

2 Single object

To model floating objects whose vertical position cannot vary, we use a similar approach to Vella *et al.* considering vertical infinite plates immersed in a liquid.[14] We consider the one dimensional problem of the horizontal force between the plates by unit length. We also consider two different wetting situations for each plate (see Fig. 2). First, the liquid can be pinned at a fixed height h relative to the undisturbed surface. In this paper, we will refer to this as the "height" case. The second case is when the liquid naturally climbs along the plate with a fixed contact angle θ. We will refer to this as the "angle" case. We will show that the difference between these two wetting conditions leads to quite different interactions between large floating objects.

As we consider the interaction between two plates, each being characterized by a specific wetting condition, we will discuss about the three different cases that this situation may generate.

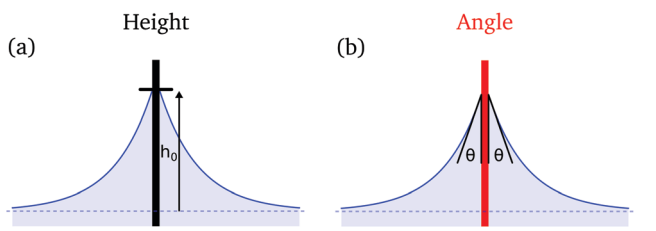

Fig. 2 Sketch of the meniscus around a vertical plate. The dashed horizontal line is the elevation of the water far away from the plates. Two different plates are considered. (a) The contact line is pinned at a defined height h_0. (b) The contact angle θ is fixed along the plate.

First, we will focus on a single plate, computing the shape of the meniscus along the plate and showing that any horizontal capillary force cannot appear on a single object. Secondly, we will consider the interaction between two plates, computing the shape of the meniscus and the force between two plates and discussing the appearance of an equilibrium distance between them supported by experimental observations.

2.1 Pressure balance

We first compute the shape of the meniscus $h(x)$ around a single plate. The result will be exploited in the following section. This shape is given by the balance between the hydrostatic pressure and the Laplace pressure along the liquid–air interface

$$\rho g h(x) = \gamma\left(\frac{1}{R_1} + \frac{1}{R_2}\right), \tag{1}$$

where ρ is the density of the liquid, g is the gravity, γ is the surface tension, and R_1 and R_2 are the two principal radii of curvature. As the meniscus climbs along an infinite plate, one of these radii diverges and the other one is given by

$$R(x) = \left|\frac{\left(1 + \left(\frac{\mathrm{d}h}{\mathrm{d}x}\right)^2\right)^{\frac{3}{2}}}{\frac{\mathrm{d}^2h}{\mathrm{d}x^2}}\right|. \tag{2}$$

By considering low deformation we can consider that $\frac{\mathrm{d}h}{\mathrm{d}x} \ll 1$. Thus, the radius of curvature reduces to

$$\frac{1}{R(x)} = \frac{\mathrm{d}^2h}{\mathrm{d}x^2}. \tag{3}$$

With the introduction of the capillary length: $l_c = \sqrt{\frac{\gamma}{\rho g}}$, eqn (1) reduces to

$$\frac{\mathrm{d}^2h(x)}{\mathrm{d}x^2} - \frac{1}{l_c^2}h(x) = 0, \tag{4}$$

which is a second order, linear, homogeneous differential equation. The latter admits the following general solution

$$h(x) = C_1 \mathrm{e}^{-\frac{x}{l_c}} + C_2 \mathrm{e}^{\frac{x}{l_c}}, \tag{5}$$

where C_1 and C_2 are constant lengths that can be determined by using the right boundary conditions.

2.2 Boundary conditions

We can assume that far away from the plate, the height of the liquid h is not influenced by the presence of the plate. Thus, we can assume the following condition $h(\infty) = 0$ leading to a fixed value of the constant $C_2 = 0$.

To find the value of C_1 we need to consider the wetting conditions on the plate. For the case of a pinned meniscus at a determined height h_0, shown in Fig. 2(a), the boundary condition along the plate must be $h(0) = h_0$. This condition sets the value of the constant $C_1 = h_0$. This gives the equation for the meniscus pinned along the plate at a fixed height h_0. One has

$$h(x) = h_0 \mathrm{e}^{-\frac{x}{l_c}}. \tag{6}$$

For the case of a meniscus contacting the plate with a determined contact angle θ, shown in Fig. 2(b), the boundary condition along the plate must be

$$\left.\frac{\mathrm{d}h}{\mathrm{d}x}\right|_{x=0} = -\cot\theta. \tag{7}$$

This condition set the value of the constant at $C_1 = l_c \cot\theta$. This gives

$$h(x) = l_c \cot\theta \mathrm{e}^{-\frac{x}{l_c}}, \tag{8}$$

as the meniscus equation along the plate for a determined contact angle.

2.3 Force on a single plate

The horizontal capillary force on a single vertical plate could be caused by two different effects. First, when the meniscus on each side reaches the plate at different heights, a pressure difference appears between the sides of the plate. This effect causes a net force on the plate. As explained in ref. 14, the horizontal component by unit length of this force can be written as $F_P = \frac{1}{2}\rho g\left(h_l^2 - h_r^2\right)$, where h_l end h_r are the heights of the meniscus for respectively the left and the right sides of the plate.

Secondly, if the contact angle of the meniscus is different on each side of the plate, an asymmetry can appear between the surface tension forces acting on each side. This effect also causes a force on the plate. The horizontal component of this force can be written as the difference between the horizontal projection of the surface tension force on each side: $F_\gamma = \gamma(\cos\phi_l - \cos\phi_r)$ where ϕ_l and ϕ_r are the angles between the horizontal and respectively the left and right menisci on each side of the plate. Considering only vertical plates, $\phi = \frac{\pi}{2} - \theta$.

The total horizontal force by unit length $F_P + F_\gamma$ on the plate is therefore

$$F_h = \frac{1}{2}\rho g\left(h_l^2 - h_r^2\right) + \gamma(\cos\phi_l - \cos\phi_r). \tag{9}$$

If we consider small liquid deformations caused by the plate, we can use the small-angle approximation. This allows us to consider that $\cos\phi \simeq -\frac{1}{2}\tan^2\phi + 1$. Thus, the horizontal force can be approximated as

$$F_h = \frac{\gamma}{2l_c^2}\left(h_l^2 - h_r^2 + l_c^2\tan^2\phi_r - l_c^2\tan^2\phi_l\right). \tag{10}$$

In the case of a pinned meniscus, using eqn (6), we see that

$$\tan\phi_i = \left.\frac{\mathrm{d}h}{\mathrm{d}x}\right|_{x=0} = -\frac{h_i}{l_c}, \tag{11}$$

with i = {l, r} denoting the considered side of the plate and $x = 0$ corresponding to the horizontal position of the plate.

In the case of the contact angle, using eqn (8), we see that

$$h_i = l_c \cot\theta_i = l_c \tan\phi_i, \tag{12}$$

with i = {l, r}.

These results show that the contact height h_i and the contact angle θ_i of a meniscus along a vertical plate are always linked together and thus, giving eqn (10), a horizontal capillary force on a single vertical plate cannot appear.

3 Two objects

3.1 Meniscus between two plates

To compute the shape of a meniscus hanging between two plates separated by a distance L, we use eqn (5) again, introducing boundary conditions.

We consider the first case where a meniscus is pinned on each plate at a determined height h_1 for the left plate and h_2 for the right plate (see Fig. 3(a and b)). Thus, the boundary condition is $h(0) = h_1$ for the left plate and $h(L) = h_2$ for the right plate.

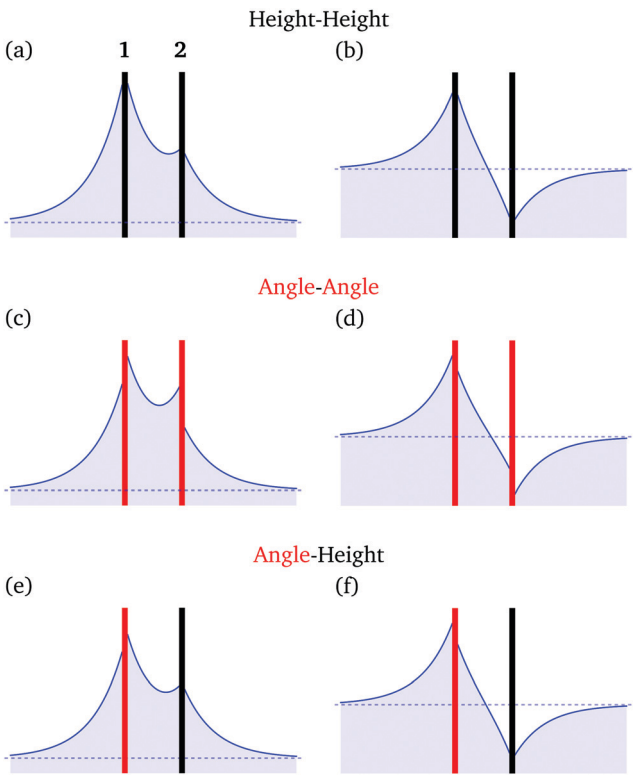

Fig. 3 Profiles, mathematically obtained, of the menisci between two plates. The contact lines are pinned on the two black plates in (a) and (b), with capillary charges of the same sign and opposite signs respectively. The contact angle is fixed on the two red plates in (c) and (d), with capillary charges of the same sign and opposite signs respectively. In (e) and (f), the contact angle is fixed on the red plate while the contact line is pinned on the black plate, and the capillary charges have the same sign and opposite signs respectively.

These boundary conditions give the following equation for the shape of the meniscus in between the plates

$$h(x) = \frac{h_1 \sinh\left(\frac{L-x}{l_c}\right) + h_2 \sinh\left(\frac{x}{l_c}\right)}{\sinh\left(\frac{L}{l_c}\right)}. \tag{13}$$

We now consider the second case where a meniscus is in contact with each plate with a determined contact angle θ_1 for the left plate and θ_2 for the right plate (see Fig. 3(c and d)). Thus, the boundary condition is $\left.\frac{dh}{dx}\right|_{x=0} = -\cot\theta_1$ for the left plate and $\left.\frac{dh}{dx}\right|_{x=L} = \cot\theta_2$ for the right plate.

These boundary conditions give the following equation for the shape of the meniscus between the plates

$$h(x) = \frac{l_c \cot\theta_1 \cosh\left(\frac{L-x}{l_c}\right) + l_c \cot\theta_2 \cosh\left(\frac{x}{l_c}\right)}{\sinh\left(\frac{L}{l_c}\right)}. \tag{14}$$

We consider a third case where a meniscus is in contact with the left plate with a contact angle θ_1 while the other one is pinned on the right plate at a determined height h_2 (see Fig. 3(e and f)). Thus, the boundary condition is $\left.\frac{dh}{dx}\right|_{x=0} = -\cot\theta_1$ for the left plate and $h(L) = h_2$ for the right plate. These boundary conditions give the following equation for the shape of the meniscus between the plates

$$h(x) = \frac{l_c \cot\theta_1 \sinh\left(\frac{L-x}{l_c}\right) + h_2 \cosh\left(\frac{x}{l_c}\right)}{\cosh\left(\frac{L}{l_c}\right)}. \tag{15}$$

3.2 Force between two plates

3.2.1 Relevance of the meniscus outside the plates. To simplify subsequent calculations, we will first show that the horizontal force between two plates does not depend on the shape of the menisci outside the plates and therefore depends only on the shape of the meniscus between the plates.

According to the Newton's law of action–reaction, the horizontal force on each plate must be of the same magnitude but in opposite directions. Thus, we only need to compute the force on one of the two plates. Using eqn (10), the horizontal force by unit length on the left plate can be written as

$$F_h = \frac{\gamma}{2l_c^2}\left(h_{out}^2 - h_{in}^2 + l_c^2 \tan^2\phi_{in} - l_c^2 \tan^2\phi_{out}\right), \tag{16}$$

where h_{out} and h_{in} are respectively the contact heights of the meniscus outside of the plates and inside of the plates. Angles ϕ_{out} and ϕ_{in} denote respectively the angles of the meniscus for both situations. This equation is tuned so that the force is negative when attractive and positive when repulsive.

As we can consider that the meniscus outside the plates is not modified by the second plate, the meniscus on the outside of the plates is the same as the meniscus along a single plate. It allows us to use the relation linking the contact height and the contact angle along a single plate (eqn (12)), to write

$$h_{\text{out}} = l_c \tan \phi_{\text{out}}. \tag{17}$$

This result leads to the following equation:

$$F_h = \frac{\gamma}{2l_c^2}\left(l_c^2 \tan^2 \phi_{\text{in}} - {h_{\text{in}}}^2\right) \tag{18}$$

In this equation only terms relative to the meniscus inside the plates remain, meaning that only the shape of the meniscus between two plates is relevant in the computation of the horizontal force. We can also see that two terms remain, one containing the contact angle of the meniscus along the plate and the other one the height of the meniscus along the plate, one of the two being constant depending on the studied case. For the case of a "height" plate, as the pinning height along the plate is constant, this equation shows that the force is caused by the variation of the contact angle along the plate when a second plate approaches. For the case of an "angle" plate, as the contact angle along the plate is constant, the force is caused by the variation of the contact height of the meniscus when a second plate approaches.

3.2.2 First case: "height–height". We first compute the force between two plates with a pinning condition separated by a distance L. The position of the left plate corresponds to the origin of the x-axis. We use eqn (18) to compute the horizontal force on the left plate. As we consider the case of a determined pinning height along the plate, we can see on Fig. 3(a and b) that the contact height is the same on each side of the plate while the contact angle of the meniscus varies from one side to the other. Therefore, the horizontal force originates from this angle difference.

The angle ϕ_1 between the horizontal and the meniscus along the left plate is determined by using the relationship $\tan \phi_1 = \left.\frac{dh}{dx}\right|_{x=0}$ where $h(x)$ is the meniscus profile given by eqn (13). Thus, eqn (18) becomes

$$\tan \phi_1 = \left.\frac{dh}{dx}\right|_{x=0} = \frac{h_2 - h_1 \cosh\left(\frac{L}{l_c}\right)}{l_c \sinh\left(\frac{L}{l_c}\right)}, \tag{19}$$

where h_1 and h_2 are respectively the pinning height of the meniscus on the left and right plates. Then, the force can be written as

$$F_h = \frac{\gamma}{2l_c^2}\left[\left(\frac{h_2 - h_1 \cosh\left(\frac{L}{l_c}\right)}{\sinh\left(\frac{L}{l_c}\right)}\right)^2 - {h_1}^2\right]. \tag{20}$$

To simplify the latter equation, we take inspiration from the notion of capillary charge introduced by Kralchevsky.[17] The capillary charge of an object is related to the vertical deformation of the interface along the object. As these charges are originally defined for circular objects, we have to use a 1D analogy of this concept. In the case of an infinite plate, we consider that the capillary charge corresponds directly to the vertical deformation of the liquid along the object. We define Q_1 as the capillary charge of the left plate and Q_2 the capillary charge of the right plate as

$$\begin{aligned} Q_1 &= h_1 \\ Q_2 &= h_2. \end{aligned} \tag{21}$$

We can then rewrite the equation of the horizontal force per unit length F_h nondimensionalized by the surface tension γ so that Q_1 and Q_2 have similar roles

$$\frac{F_h}{\gamma} = \frac{1}{l_c^2 \sinh^2\left(\frac{L}{l_c}\right)}\left[\frac{\left({Q_1}^2 + {Q_2}^2\right)}{2} - Q_1 Q_2 \cosh\left(\frac{L}{l_c}\right)\right]. \tag{22}$$

Using a similar method to compute the horizontal force on the right plate gives the same result, as expected from the Newton's law of action–reaction.

Note that the force is not given by a simple product of capillary charges. As a result, the behaviour is more complex than the usual attraction between charges of the same sign and repulsion between opposite signs. As the force is attractive when negative and repulsive when positive, we can see on Fig. 4(a) that when the capillary charges of two plates are of the same sign, meaning the liquid deformation is on the same direction, the force is attractive at long range and repulsive at short range, which brings up a stable equilibrium distance. When two plates have capillary charges of opposite signs, we can see from Fig. 4(b) that the force is always repulsive. Also, when both capillary charges are the same in absolute value, we find the classical case of an attraction between the same sign and repulsion between opposite signs.

A more surprising result appears when we consider one of the capillary charges equal to zero. This can happen for example when the meniscus is pinned at the height of the free surface. In this particular case, the second term of eqn (22) becomes zero but the first term remains. As a result, an interaction can occur with a zero charge. Note that as the meniscus is pinned, a zero charge is different than the absence of charge. This interaction between a charge Q and a neutral charge is given by

$$\frac{F_h}{\gamma} = \frac{Q}{2}\operatorname{csch}^2\left(\frac{L}{l_c}\right), \tag{23}$$

note that this equation is always positive, meaning that the interaction is always repulsive in that case.

3.2.3 Second case: "angle–angle". We use eqn (18) to compute the horizontal force on the left plate. As we consider the case of a fixed contact angle along the plate, the angular term $l_c^2 \tan^2 \phi$ stays constant while the height of the meniscus varies (see Fig. 3(c and d)). In this case, the horizontal force originates from the pressure difference on the plates.

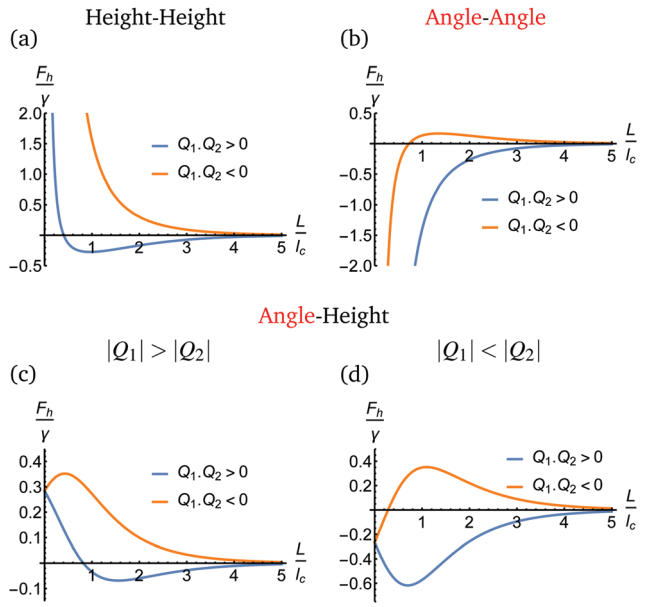

Fig. 4 Plots of the horizontal force by unit of length between two vertical plates divided by the surface tension as a function of the ratio between the spacing L of those plates and the capillary length l_c, with $|Q_1| \neq |Q_2|$. (a) and (b) Show this force between two "height" plates and two "angle" plates respectively. (c) and (d) Show this force between a "height" plate and an "angle" plate when the capillary charge caused by the "height" plate is larger than the one caused by the "angle plate" and the opposite case, respectively. The orange and the blue curves show this force when the capillary charges have the same signs and opposite signs respectively.

The height of the meniscus along the plate $h(0)$ is determined by using the meniscus profile eqn (14). One has

$$h(0) = \frac{l_c \cot\theta_1 \cosh\left(\frac{L}{l_c}\right) + l_c \cot\theta_2}{\sinh\left(\frac{L}{l_c}\right)}, \quad (24)$$

where θ_1 and θ_2 are respectively the contact angles of the meniscus on the left and right plates. Then, the force can be written as

$$F_h = \frac{\gamma}{2l_c^2}\left[l_c^2 \tan^2\phi_1 - \left(\frac{l_c \cot\theta_1 \cosh\left(\frac{L}{l_c}\right) + l_c \cot\theta_2}{\sinh\left(\frac{L}{l_c}\right)}\right)^2\right] \quad (25)$$

which has been previously obtained by Vella *et al.*[14] In this case, we define Q_1 as the capillary charge of the left plate and Q_2 as the capillary charge of the right plate. One has

$$\begin{aligned} Q_1 &= l_c \cot\theta_1, \\ Q_2 &= l_c \cot\theta_2. \end{aligned} \quad (26)$$

The relation between the contact angle and the contact height of the meniscus along a plate (eqn (12)) shows that whatever the wetting condition, the capillary charge is related to the vertical deformation of the meniscus.

We can then rewrite the equation of the horizontal force per unit length F_h nondimensionalized by the surface tension γ

$$\frac{F_h}{\gamma} = \frac{1}{l_c^2 \sinh^2\left(\frac{L}{l_c}\right)}\left[-\frac{(Q_1^2 + Q_2^2)}{2} - Q_1 Q_2 \cosh\left(\frac{L}{l_c}\right)\right], \quad (27)$$

where Q_1 and Q_2 play a similar role. As with the previous case and in agreement with the law of action–reaction, using a similar method to compute the horizontal force on the right plate gives the same result. This force is always attractive when the capillary charges have the same sign. When the charges have opposite signs, the situation is more complex and we see a long range repulsion and a short range attraction with an unstable equilibrium distance between them (see Fig. 4(c and d)). This behaviour is the exact opposite of the previous case, which shows the importance of taking into account the condition of contact of the liquid on the object.

Also, similarly to the previous case, when both capillary charges are the same in absolute value, we find the classical case of an attraction between same sign and repulsion between opposite signs.

When we consider a neutral capillary charge, occurring when the contact angle of one plate is equal to 90°, the second term of eqn (27) becomes zero but the first term remains. As a result, an interaction can occur with a neutral charge. Note that as the contact angle of the meniscus is fixed, a zero charge is different to the absence of charge. This interaction is given by

$$\frac{F_h}{\gamma} = -\frac{Q}{2}\mathrm{csch}^2\left(\frac{L}{l_c}\right), \quad (28)$$

where Q is the value of the non-zero charge. Note that as opposed to the previous case, this interaction is always attractive.

3.2.4 Third case: "angle–height". We compute the horizontal force between two vertical plates for the third case where a meniscus is in contact with the left plate with a contact angle θ_1 and pinned on the right plate at a determined height h_2. We use eqn (18) to compute the horizontal force on the left plate. In this case, the left plate is the one with an angle condition so when we consider a fixed contact angle along the plate, the angular term $l_c^2 \tan^2\phi_1$ stays constant while the height of the meniscus varies. So for this plate the force is caused by a pressure difference.

The height of the meniscus along the left plate $h(0)$ is determined by using the meniscus profile equation (eqn (15)). One has

$$h(0) = \frac{l_c \cot\theta_1 \sinh\left(\frac{L}{l_c}\right) + h_2}{\cosh\left(\frac{L}{l_c}\right)}, \quad (29)$$

where θ_1 is the contact angle of the liquid on the left plate and h_2 is the pinning height of the meniscus along the right plate.

Then, the force can be written as

$$F_h = \frac{\gamma}{2l_c^2}\left[l_c^2 \tan^2\phi_1 - \left(\frac{l_c \cot\theta_1 \sinh\left(\frac{L}{l_c}\right) + h_2}{\cosh\left(\frac{L}{l_c}\right)}\right)^2\right]. \quad (30)$$

Similarly to a previous case, we introduce the capillary charges as

$$\begin{aligned} Q_1 &= l_c \cot\theta_1, \\ Q_2 &= h_2. \end{aligned} \quad (31)$$

Then we rewrite the equation of the horizontal force per unit length F_h nondimensionalized by the surface tension γ where Q_1 and Q_2 play a similar role. One has

$$\frac{F_h}{\gamma} = \frac{1}{l_c^2 \cosh^2\left(\frac{L}{l_c}\right)}\left[\frac{(Q_1^2 - Q_2^2)}{2} - Q_1 Q_2 \sinh\left(\frac{L}{l_c}\right)\right]. \quad (32)$$

In this case we computed the force on the left plate. This force is caused by a pressure difference. The origin of the force on the right plate is different as it is caused by the contact angle difference on the plate. However, as with the previous cases, using a similar method to compute the horizontal force on the right plate gives the same result thanks to the action–reaction principle.

We observe on Fig. 4(c and d) that the behaviour of the force is more complicated than in the two previous cases. The behaviour not only changes completely when the capillary charges have the same signs or different signs but also depends on which plate has the larger capillary charge in absolute value. We can see from Fig. 4(c) that when the charge of the ''angle'' plate Q_1 is larger than the charge of the ''height'' plate Q_2 (in absolute value), and the charges have the same signs, we have a long range attraction with a short range repulsion separated by a stable equilibrium distance. On the other hand, when the charges have opposite signs the force is always repulsive. When the charge of the ''height'' plate Q_2 is bigger than the charge of the ''angle'' plate Q_1, we see on Fig. 4(d) that when the charges have the same signs the force is always attractive. However, when the charges have opposite signs the force is repulsive at long range and attractive at short range leading to an unstable equilibrium distance.

Also, similar to previous cases, when both capillary charges are the same in absolute value, we find the classical case of an attraction between the same sign and repulsion between opposite signs.

Considering a zero charge forces us to differentiate between two cases. When the ''height'' charge is zero, *i.e.* when the meniscus is pinned at the height of the undisturbed surface, the interaction is given by

$$\frac{F_h}{\gamma} = \frac{Q}{2}\mathrm{sech}^2\left(\frac{L}{l_c}\right), \quad (33)$$

leading to a repulsion. When the ''angle'' charge is zero, *i.e.* when the contact angle of the ''angle'' plate is equal to 90°, the interaction is given by

$$\frac{F_h}{\gamma} = -\frac{Q}{2}\mathrm{sech}^2\left(\frac{L}{l_c}\right), \quad (34)$$

leading to an attraction.

We see that without consideration for the second plate, a zero ''height'' capillary charge is always repulsive while a zero ''angle'' charge is always attractive. This result is of the utmost importance in areas such as the capillary self-assembly of floating objects where a new type of interaction could allow us to achieve new complex structures.

3.3 Equilibrium distance

3.3.1 First case: ''height–height''. We can see that for each of the different cases, specific conditions on the capillary charges allow the existence of an equilibrium distance between the plates. The equilibrium distance is stable in some cases and unstable in others. We can compute the equilibrium distance for each case using the respective force equation, but we can also find the expression of these equilibrium distances using a more intuitive method that gives a better insight into what causes this equilibrium to appear.

For the first case, the equilibrium distance between two ''height'' plates is always stable and appears only when two plates possess capillary charges of the same signs. We can inverse analytically eqn (22) to find the distance that gives a force equal to zero. This gives the following equilibrium distance

$$L_{eq} = l_c\left|\ln\left(\frac{Q_1}{Q_2}\right)\right|. \quad (35)$$

The equilibrium distance increases with the ratio between the capillary charges and tends toward zero when the charges become similar, which is compatible with the behaviour observed in previous studies.[2–8,13–18] Looking at the meniscus in this situation helps to better understand the cause of the appearance of an equilibrium and gives the same calculation result. In Fig. 5(a), we see that when the plates are separated by some equilibrium distance, the meniscus of the left plate with the larger capillary charge is not perturbed by the right one. Therefore, the right plate does not modify the contact angle on the left plate so no force is exerted on the plate. Looking at the right plate, we can see that even if the contact angle of the meniscus along the plate is perturbed by the left plate, the angle between the meniscus and the horizontal stays the same in absolute value cancelling the horizontal force on this plate too.

We can use these observations to compute the equilibrium distance again. In this case, the shape of the undisturbed meniscus is derived from eqn (6). At the equilibrium distance, the height of the undisturbed meniscus along the left plate is equal to the pinning height of the meniscus along the right

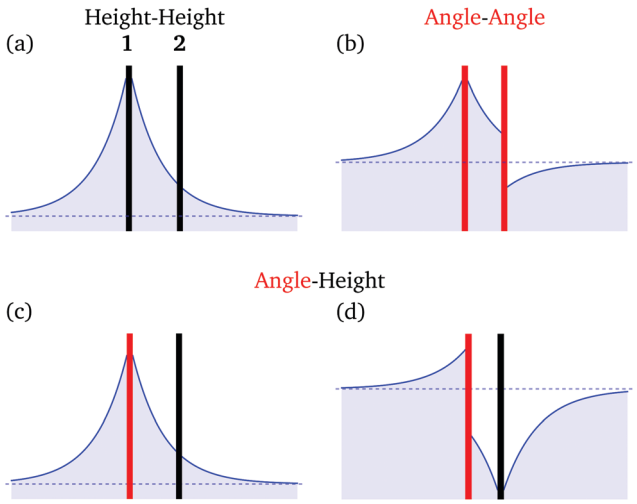

Fig. 5 Profiles mathematically obtained of the menisci between two plates at equilibrium. (a) and (b) Show the case of the stable equilibrium between two "height" plates and the case of two "angle" plates respectively. (c) and (d) Show the case of an "angle" and a "height" plate for capillary charges of the same signs and opposites signs respectively.

plate. Introducing this in eqn (6) allows us to find the same result for the equilibrium distance as from eqn (35).

3.3.2 Second case: "angle–angle". For the second case, the equilibrium distance between two "angle" plates is always unstable and appears only when the two plates have capillary charges of opposite signs. We can inverse analytically eqn (27) to find the distance that gives a force equal to zero. This gives the following equilibrium distance

$$L_{eq} = l_c \left| \ln\left(-\frac{Q_1}{Q_2}\right) \right|. \tag{36}$$

We can see that, as in the first case, the equilibrium distance increases with the ratio between the absolute value of the capillary charges and tends toward zero when the charges are the same.

In Fig. 5(b), we see that when the plates are separated by the equilibrium distance, the meniscus of the left plate with the larger capillary charge is not perturbed by the right plate. Therefore, the right plate does not modify the contact height on the left plate so no force is exerted on the plate. Looking at the right plate, we can see that even if the meniscus along the plate is perturbed by the left plate, the contact height of the meniscus along the plate stays the same in absolute value cancelling the horizontal force on this plate.

We can compute this considering that at the equilibrium distance, the height of the meniscus of the left plate is the same as the height of the meniscus for a single plate. Equating eqn (8) and eqn (14) for $x = 0$ gives us an equation for the equilibrium distance similar to eqn (36).

3.3.3 Third case: "angle-height". For the third case, an equilibrium distance between a left "angle" plate and a right "height" plate can appear in two different situations. First, a stable equilibrium distance appears when the two plates have capillary charges of the same sign with the charge of the "angle" plate larger in absolute value than the charge of the "height" plate. Secondly, an unstable equilibrium distance appears when the two plates have capillary charges of opposite signs with the charge of the "height" plate larger in absolute value then the charge of the "angle" plate. We can inverse analytically eqn (32) to find the distance that gives a force equal to zero. This gives the following equilibrium distance:

$$\begin{aligned} L_{eq} &= l_c \ln\left(\frac{Q_1}{Q_2}\right) \text{ if } |Q_1| > |Q_2|, \\ L_{eq} &= l_c \ln\left(-\frac{Q_2}{Q_1}\right) \text{ if } |Q_2| > |Q_1|. \end{aligned} \tag{37}$$

We can see that the equilibrium distance still increases with the ratio between the absolute value of the capillary charges and tends toward zero when the charges become similar.

In Fig. 5(c), we see that when the plates are separated by the equilibrium distance, the meniscus of the left plate with the larger capillary charge is not perturbed by the right plate. Therefore, the right plate does not modify the contact height of the meniscus on the left plate so no force is exerted on the plate. Looking at the right plate, we can see that even if the contact angle of the meniscus along the plate is perturbed by the left plate, the angle between the meniscus and the horizontal stays the same in absolute value cancelling the horizontal force on this plate.

In Fig. 5(d), we see that when the plates are separated by the equilibrium distance, by looking at the left plate, we can see that even if the meniscus along the plate is perturbed by the right plate, the contact height of the meniscus along the plate stays the same in absolute value cancelling the horizontal force on the plate. We can also see that the meniscus created by the right plate with the larger capillary charge is not perturbed by the left plate. Therefore, the left plate does not modify the contact angle on the right plate so no force is exerted on the plate.

The equation for the equilibrium distance can be generalized using the following form

$$L_{eq} = l_c \ln\left(\frac{\max\{|Q_1|, |Q_2|\}}{\min\{|Q_1|, |Q_2|\}}\right), \tag{38}$$

which holds for all different cases. This last equation represents the major result of our work.

4 Experiments

Using eqn (38), we are able to predict the equilibrium distance in configurations like the one shown in Fig. 1(a) where two large floating objects are pinning the meniscus at different heights. This corresponds to the "height–height" case we studied before. This case gives a stable equilibrium distance between two objects of different capillary charges but of the same sign, which explains what can be seen in Fig. 1(a). Therefore, we built an experimental setup to measure precisely the equilibrium distance in this case. The setup, as sketched in Fig. 6 is composed of a water tank, with a mobile floating object

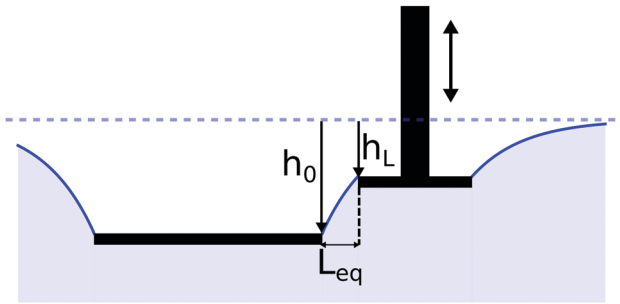

Fig. 6 Sketch of the experiment. On the left is the floating object pinning the meniscus at a depth h_0, on the right is the fixed object pinning the meniscus at a variable depth h_L. We measure the equilibrium distance L_{eq} between both objects.

(shown on the left) and a fixed object (shown on the right). It should be remembered that a large non-buoyant object could sink depending on its shape and density. Anyway, this can occur at sizes large enough in relation to the capillary length that it is still possible to have a large size range of objects with no variation of their vertical position.

The mobile object is freely floating at its natural floating depth h_0. This object is a 3D-printed ABS rectangle: Thickness 0.2 cm, width 6 cm and length 20 cm. Its size which is large compared to the capillary length, allows for neglecting any tilt or height change of the object. We assume that the rectangle is perfectly horizontal. We built two rectangles. Their weight is adjusted by adding material at the center of their surface to ensure that one is naturally floating at a depth $h_0 \approx l_c/3$ and the second one at a depth $h_0 \approx l_c/2$. The fixed object is a 3D-printed rectangle 6 cm wide and 3 cm long attached to a vertical precision screw. This object pins the meniscus at a depth h_L. Both objects have a sharp edge to force the pinning of the meniscus at a precise height. A camera is placed above the water to measure precisely the distance L_{eq} between objects. The rectangle is gently placed on the surface of distilled water close to the fixed object. The depth of the fixed object is controlled manually with the precision screw so that it attracts the moving object. The depth is increased until the maximum depth is reached, before the water covers the object. Then the depth of the fixed object is reduced in 50 μm steps until the undisturbed surface is reached. At each step, we wait a few seconds until the object stabilizes in its equilibrium position before taking a picture. This method allowed us to measure the equilibrium distance L_{eq} as a function of the depth of the fixed part h_L for both rectangles. The experiment is repeated ten times for each rectangle and the results are averaged to reduce variance.

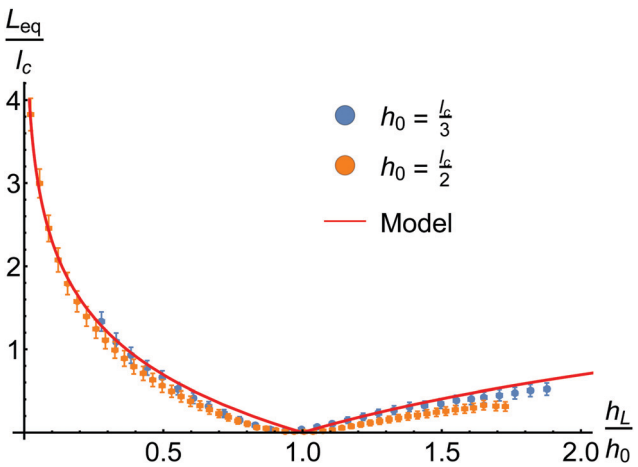

Fig. 7 Graph of the ratio between the equilibrium distance and the capillary length as a function of the ratio between the depth of the fixed object and the depth of the moving object. The red curve corresponds to the theoretical model while the blue and orange dots correspond to the experiment for a floating object hanging the meniscus at a depth of $l_c/3$ and $l_c/2$ respectively.

The results are shown in Fig. 7. We plotted the depth of the fixed part h_L divided by the depth of the mobile part h_0 on the x-axis, and the equilibrium distance L_{eq} divided by the capillary length l_c on the y-axis in order to condense our data. The dots are the experimental data with error bars, while the red curve corresponds to the theoretical model. We can observe a good agreement between data and model (eqn (38)). Moreover, the model is able to predict that the objects come into contact ($L_{eq} = 0$) when depths become equivalent ($h_L \approx h_0$).

5 Conclusions

In this article we have shown that the interaction between floating objects on a free surface is more complex than previously assumed. We focused on objects whose floating depth does not vary, either because of their size or because of the presence of other objects around them. The origin of the interaction between such objects does not result from gravity or buoyancy as would be expected for smaller objects. Moreover, we provided experimental observations that couldn't be explained using the usual arguments. For these reasons, we proposed a different view based solely on the shape of the meniscus caused by the floating objects. More precisely, the meniscus between the objects as the outer meniscus has no effect according to eqn (18). We computed the horizontal force per unit length between vertical plates and showed that the behaviour of this force is more complex than just an attraction between capillary charges of the same sign or a repulsion between capillary charges of opposite signs. We have shown that, in most typical cases, attraction and repulsion can appear depending on the distance between the objects leading to stable or unstable equilibrium distances between them. We show that the wetting condition of the meniscus along the object is of utmost importance. We have defined two different conditions; the meniscus can be pinned along the object at a fixed height, we called this the "height" case. In a second case, the meniscus can contact the object with a fixed contact angle, we called this the "angle" case. We have shown that the behaviour of the force and the apparition of the equilibrium depends entirely on this wetting condition. Thus, we show that the capillary charge introduced by Kralchevsky[16–18] is not

sufficient to fully account for the behaviour of the interaction between objects at the surface of a liquid. The capillary charge of the object needs to be completed by the wetting condition, ''height'' or ''angle''. We also show that objects may interact with other objects of zero capillary charge. This counter-intuitive result means that a zero capillary charge and the absence of capillary charge are two different situations. We have provided an intuitive explanation for the apparition of the equilibrium distance as well as a general equation to predict it (eqn (38)). We also gave experimental confirmation of the validity of this equation.

These are important results for the fundamental understanding of the phenomenon, which may allow for further development in the field of capillary self-assembly of floating objects.

Conflicts of interest

There are no conflicts to declare.

Acknowledgements

This work has been financially supported by the CESAM Research Unit from the University of Liège.

Notes and references

1 M. Nicolson, *Mathematical Proceedings of the Cambridge Philosophical Society*, 1949, pp. 288–295.
2 G. M. Whitesides and B. Grzybowski, *Science*, 2002, **295**, 2418–2421.
3 N. Bowden, A. Terfort, J. Carbeck and G. M. Whitesides, *Science*, 1997, **276**, 233–235.
4 N. Bowden, S. R. Oliver and G. M. Whitesides, *J. Phys. Chem. B*, 2000, **104**, 2714–2724.
5 P. W. Rothemund, *Proc. Natl. Acad. Sci. U. S. A.*, 2000, **97**, 984–989.
6 M. Berhanu and A. Kudrolli, *Phys. Rev. Lett.*, 2010, **105**, 098002.
7 N. Vandewalle, N. Obara and G. Lumay, *Eur. Phys. J. E: Soft Matter Biol. Phys.*, 2013, **36**, 1–6.
8 M. Poty, G. Lumay and N. Vandewalle, *New J. Phys.*, 2014, **16**, 023013.
9 G. Lumay, N. Obara, F. Weyer and N. Vandewalle, *Soft Matter*, 2013, **9**, 2420–2425.
10 G. Grosjean, M. Hubert, Y. Collard, S. Pillitteri and N. Vandewalle, *Eur. Phys. J. E: Soft Matter Biol. Phys.*, 2018, **41**, 1–10.
11 D. L. Hu and J. W. Bush, *Nature*, 2005, **437**, 733–736.
12 J. Voise, M. Schindler, J. Casas and E. Raphaël, *J. R. Soc., Interface*, 2011, **8**, 1357–1366.
13 W. Gifford and L. Scriven, *Chem. Eng. Sci.*, 1971, **26**, 287–297.
14 D. Vella and L. Mahadevan, *Am. J. Phys.*, 2005, **73**, 817–825.
15 H. Cooray, P. Cicuta and D. Vella, *J. Phys.: Condens. Matter*, 2012, **24**, 284104.
16 P. A. Kralchevsky and K. Nagayama, *Langmuir*, 1994, **10**, 23–36.
17 P. A. Kralchevsky and N. D. Denkov, *Curr. Opin. Colloid Interface Sci.*, 2001, **6**, 383–401.
18 K. D. Danov, P. A. Kralchevsky, B. N. Naydenov and G. Brenn, *J. Colloid Interface Sci.*, 2005, **287**, 121–134.
19 I. Ho, G. Pucci and D. M. Harris, *Phys. Rev. Lett.*, 2019, **123**, 254502.
20 D. M. Harris, J. Quintela, V. Prost, P.-T. Brun and J. W. Bush, *J. Visualization*, 2017, **20**, 13–15.
21 N. Vandewalle, M. Poty, N. Vanesse, J. Caprasse, T. Defize and C. Jérôme, *Soft Matter*, 2020, **16**, 10320–10325.
22 H. N. Dixit and G. Homsy, *Phys. Fluids*, 2012, **24**, 122102.
23 J.-C. Loudet, A. G. Yodh and B. Pouligny, *Phys. Rev. Lett.*, 2006, **97**, 018304.
24 E. Mansfield, H. Sepangi and E. Eastwood, *Philos. Trans. R. Soc., A*, 1997, **355**, 869–919.
25 P. A. Kralchevsky, V. N. Paunov, N. D. Denkov and K. Nagayama, *J. Colloid Interface Sci.*, 1994, **167**, 47–65.